12.3 OBSERVATIONS OF THE FORMATION OF LOW-LEVEL ROTATION: THE 5 JUNE 2001 SUMNER COUNTY, KANSAS TORNADO

David C. Dowell[1], Yvette P. Richardson[2], Joshua M. Wurman[3]
[1] National Center for Atmospheric Research*, Boulder, CO
[2] Department of Meteorology, The Pennsylvania State University, University Park, Pennsylvania
[3] School of Meteorology, University of Oklahoma, Norman, OK

1. INTRODUCTION

Evidence from numerical simulations (Klemp and Rotunno 1983; Lewellen 1993; Wicker and Wilhelmson 1995) and visual observations indicates that mesocyclones and tornadoes are features that evolve rapidly (time scale ~1 min) and that have significant gradients in velocity within the lowest 1 km. Although our understanding of mesocylones and tornadoes in supercells has been improved greatly by the study of multiple-Doppler radar observations (Heymsfield 1978; Ray et al. 1981; Brandes 1984; Johnson et al. 1987; Dowell and Bluestein 1997; Wakimoto et al. 1998; Trapp 1999; Ziegler et al. 2001; Richardson et al. 2001), it was not possible with these observations to diagnose low-level mesocyclogenesis and tornadogenesis directly owing to limited spatial and temporal resolution. Previous datasets obtained from airborne and from fixed, ground-based radars typically included updates only every ~5 min and observations at only 1-2 levels in the lowest 1 km.

Two Doppler on Wheels (DOW) mobile radars (Wurman et al. 1997; Wurman 2001) collected data of unprecedented quality at low levels in a supercell thunderstorm in Sumner County, Kansas on 5 June 2001. Since the target mesocyclone was west and south-southwest of DOW2 and DOW3, respectively, the scanning geometry was favorable for dual-Doppler wind synthesis. By focusing scans on the lowest ~5 km of the storm, each radar was able to obtain volumetric data with updates approximately every 70 s. The mesocyclone and tornado were relatively close to (2-17 km away from) each radar. The radar beamwidths corresponding to these ranges were 30–280 m, and the characteristics of the flow in the lowest 1 km AGL were represented by Doppler measurements at 4 (or more) different elevation angles. During the 30 min period of coordinated dual-Doppler scanning, a low-level mesocyclone formed, and a weak tornado formed and dissipated within the mesocyclone. We describe below preliminary results from an ongoing dual-Doppler analysis of observations of the Sumner County storm.

2. FORMATION OF THE LOW-LEVEL MESOCYCLONE

When dual-Doppler scanning began, the Sumner County storm had a rather large north-south oriented reflectivity appendage on the southwest side (Fig. 1a). Within several min, the appendage had become bow shaped (Fig. 1b) after a portion of it had surged ahead. As the tornado was forming, an initially small hook echo to the north of the apex of the bow (Fig. 1b) developed into a prominent spiral in reflectivity (Fig. 1c). The hook echo appeared to be an indicator, rather than an instigator, of the developing tornado in this case.

To date, we have edited and analyzed volumetric dual-Doppler observations at 8 different times during this period of mesocyclogenesis and tornadogenesis. To interpolate the edited radar data to Cartesian grids ($\Delta x=\Delta y=\Delta z=250$ m), we used a uniform, isotropic Barnes weighting function with a smoothing parameter of 0.2 km^2. We synthesized the wind field with a traditional method employing upward integration of the continuity equation.

The dual-Doppler analysis at 0014 UTC indicates a disorganized structure with multiple updrafts at 4.0 km AGL (Fig. 2a). The northernmost of these updrafts was at the intersection of the reflectivity appendage (Fig. 1a) with the main body of the storm echo. A comparison of the analyses at 0.25 and 4.0 km AGL indicates a significant rearward (relative to the eastward storm motion) slope with height of the updraft region at the initial time (Figs. 2a and 2b). The main (north-south oriented) portion of the low-level updraft was initially linear (Figs. 2b and 2c). However, the northern flank of the low-level updraft curved sharply back toward the west beneath the northernmost mid-level updraft (Figs. 2a and 2b). The observations indicate a rather distinct difference between "laminar" flow to the east and "turbulent" flow to the west of the low-level updraft. For example, the raw Doppler velocity (not shown) and the synthesized vertical velocity (Fig. 2b) fields were rather smooth on the east side, but they contained numerous velocity perturbations ~1 km wide on the west side.

During the first several min of data collection, there was cyclonic vertical vorticity over a broad area between the gust front and the region of strong northerly outflow to its west (Figs. 3a-3c). The magnitude of vorticity tended to be greatest just behind the north-south oriented gust front, and near the northern flank of the low-level updraft that curved back toward the west.

Low-level mesocyclogenesis occurred near the gust front, in the south portion of the region that is plotted in Fig. 3. As the mesocyclone intensified, the air with relatively large values of vertical vorticity near the northern flank of the updraft appeared to be advected southward into the developing circulation (Fig. 3). The overall region of cyclonic vorticity was flanked by relatively high wind speeds (a "jet" of northerly outflow) on its west side. During future work with this case, we will test two hypotheses concerning the location of low-level mesocyclogenesis. The former is that the location of the mesocyclone was determined primarily by low-level processes. Enhanced convergence (stretching of vertical vorticity) at the intersection of the outflow jet with the gust front could have produced the local maximum in vertical vorticity near the leading left side of the jet (Fig. 3a). The latter hypothesis is that the focusing of the low-level rotation occurred in response to an intensifying updraft and mesocyclone aloft (not shown).

* The National Center for Atmospheric Research is sponsored by the National Science Foundation.

Corresponding author address: David C. Dowell, National Center for Atmospheric Research, Advanced Studies Program, P. O. Box 3000, Boulder, CO 80307-3000; ddowell@ucar.edu

During the period of mesocyclogenesis, a remarkable transition in the low-level updrafts and downdrafts occurred. While the updraft region along the northern flank dissipated, a portion of the initially linear updraft farther south developed a comma shape (Fig. 2d) that is commonly associated with tornadic supercells (Lemon and Doswell 1979; Klemp and Rotunno 1983; Wicker and Wilhelmson 1995). Furthermore, a more organized rear-flank downdraft developed in the region that was earlier more turbulent to the west and northwest of the main updraft. The tornado formed near a smaller separate downdraft (Fig. 4a), perhaps an "occlusion downdraft" (Klemp and Rotunno 1983), within the comma.

3. FORMATION OF THE TORNADO

A weak tornado formed within the mesocyclone of the Sumner County storm at approximately 0028 UTC. A sharp inbound-outbound radial velocity couplet was not apparent in the following two scans at low levels, but a tighter tornadic signature appeared again in the scans from 0031 to 0036 UTC (not shown). Since the tornado was wrapped in precipitation (Fig. 1c), no visual documentation is available. No damage was reported with this weak tornado that occurred over a plowed field. The maximum ground-relative wind speed and radial velocity difference across the couplet observed by DOW2 (the closer of the two radars) within the lowest 50 m AGL of the tornado were 38 m s^{-1} and 54 m s^{-1}, respectively (not shown). The radial velocity couplets of the tornado were associated with vertical vorticity of approximately 0.5 s^{-1} $\left(\approx 2 \times \frac{\Delta V}{\Delta L} \approx 2 \times \frac{50 \text{ m s}^{-1}}{200 \text{ m}} \right)$.

Parcel trajectories computed from the synthesized wind fields indicate that the air in the vicinity of the tornado at 250 m AGL came from two locations. One source was behind the gust front, to the north of the developing mesocyclone; the other source was ahead of the gust front, to the southeast of the developing mesocyclone (Figs. 2b-d).

To get a detailed view of features in the vicinity of the incipient tornado, we produced a dual-Doppler analysis on a finer grid (Δx=Δy=Δz=100 m) and with a smaller smoothing parameter (0.02 km^2) in the Barnes interpolation scheme. The high-resolution dual-Doppler analysis (Fig. 4) indicates that the tornado (marked with a "T") formed between the tip of the comma-shaped main low-level updraft and the downdraft inside the comma. Vertical vorticity ~0.1 s^{-1} is resolved in the dual-Doppler analysis in the location of the tornado. The vorticity maximum associated with the tornado was on the east side of a broader region of cyclonic vorticity. In addition, there was vertical vorticity >0.01 s^{-1} just behind a gust front (marked with a thick line in Fig. 4) that curved around the east, north, and west sides of the tornado.

4. CONCLUSIONS AND FUTURE WORK

The dual-DOW observations from 5 June 2001 are unique compared to previous multiple-Doppler observations of supercells in terms of the fine spatial resolution at low levels and the frequency of the scans during the period of low-level mesocyclogenesis and tornadogenesis. Preliminary analyses of the storm revealed a rapid transition from a linear low-level updraft structure to a curved updraft structure more commonly associated with tornadic storms. We are unaware of such a rapid transition documented in previous cases.

The tornado that formed in the Sumner County storm was relatively weak. In future experiments, we hope to collect additional datasets, of similar quality to those in this case, of supercells with more significant tornadoes.

In the near future, we plan to edit the remaining dual-Doppler observations of the Sumner County storm and produce syntheses of the wind field every 70 s. Animations of the derived fields, retrievals of pressure and temperature, and Lagrangian analyses of vorticity forcing terms will be possible with the complete set of wind syntheses.

ACKNOWLEDGMENTS

We appreciate the contributions of Curtis Alexander, MyShelle Bryant, Bob Conzemius, Steve McDonald, Kevin McGrath, Kevin Scharfenberg, Herb Stein, and Pengfei Zhang during ROTATE (Radar Observations of Tornadoes And Thunderstorms Experiment) 2001. We thank Jeff Trapp for comments on the paper.

REFERENCES

Brandes, E. A., 1984: Vertical vorticity generation and mesocyclone sustenance in tornadic thunderstorms: The observational evidence. *Mon. Wea. Rev*., **112**, 2253-2269.

Dowell, D. C., and H. B. Bluestein, 1997: The Arcadia, Oklahoma storm of 17 May 1981: Analysis of a supercell during tornadogenesis. *Mon. Wea. Rev*., **125**, 2562-2582.

Heymsfield, G. M., 1978: Kinematic and dynamic aspects of the Harrah tornadic storm analyzed from dual-Doppler data. *Mon. Wea. Rev*., **106**, 233-254.

Johnson, K. W., P. S. Ray, B. C. Johnson, and R. P. Davies-Jones, 1987: Observations related to the rotational dynamics of the 20 May 1977 tornadic storms. *Mon. Wea. Rev*., **115**, 2463-2478.

Klemp, J. B., and R. Rotunno, 1983: A study of the tornadic region within a supercell thunderstorm. *J. Atmos. Sci.*, **40**, 359-377.

Lemon, L. R., and C. A. Doswell, 1979: Severe thunderstorm evolution and mesocyclone structure as related to tornadogenesis. *Mon. Wea. Rev.*, **107**, 1184-1197.

Lewellen, W. S., 1993: Tornado vortex theory. *The Tornado: Its Structure, Dynamics, Prediction, and Hazards, Geophys. Monogr.*, No. 79, Amer. Geophys. Union, 19-39.

Ray, P. S., B. C. Johnson, K. W. Johnson, J. S. Bradberry, J. J. Stephens, K. K. Wagner, R. B. Wilhelmson, and J. B. Klemp, 1981: The morphology of several tornadic storms on 20 May 1977. *J. Atmos. Sci*., **38**, 1643-1663.

Richardson, Y. P., D. C. Dowell, J. M. Wurman, P. Zhang, and S. S. Weygandt, 2001: Preliminary high-resolution dual-Doppler analyses of two tornadic thunderstorms. *Preprints, 30th Conf. on Radar Meteorology*, Munich, Germany, 295-297.

Trapp, R. J., 1999: Observations of nontornadic low-level mesocyclones and attendant tornadogenesis failure during VORTEX. *Mon. Wea. Rev*., **127**, 1693-1705.

Wakimoto, R. M., C. Liu, and H. Cai, 1998: The Garden City, Kansas storm during VORTEX 95. Part I: Overview of the storm's life cycle and mesocyclogenesis. *Mon. Wea. Rev*., **126**, 372-392.

Wicker, L. J., and R. B. Wilhelmson, 1995: Simulation and analysis of tornado development and decay within a three-dimensional supercell thunderstorm. *J. Atmos. Sci*., **52**, 2675-2703.

Wurman, J., 2001: The DOW mobile multiple-Doppler network. *Preprints, 30th Conf. on Radar Meteorology*, Munich, Germany, 95-97.

Wurman, J., J. Straka, E. Rasmussen, M. Randall, and A. Zahrai, 1997: Design and deployment of a portable, pencil-beam, pulsed, 3-cm Doppler radar. *J. Atmos. Oceanic Technol.*, **14**, 1502-1512.

Ziegler, C. L., E. N. Rasmussen, T. R. Shepherd, A. I. Watson, and J. M. Straka, 2001: The evolution of low-level rotation in the 29 May 1994 Newcastle-Graham, Texas, storm complex during VORTEX. *Mon. Wea. Rev.*, **129**, 1339-1368.

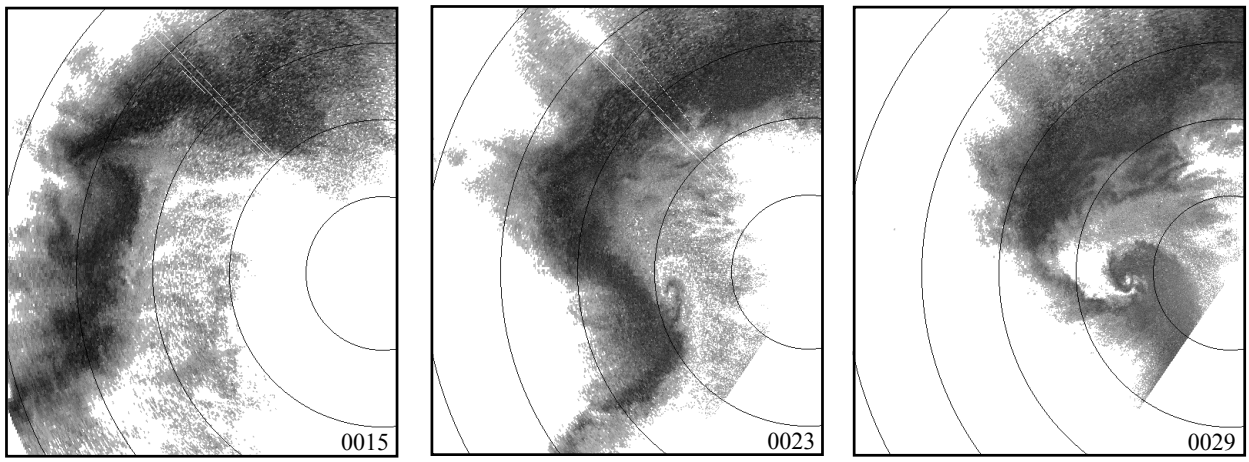

Figure 1. Reflectivity from DOW2 at (a) 0015, (b) 0023, and (c) 0029 UTC 6 June 2001. Range rings are at 5 km intervals.

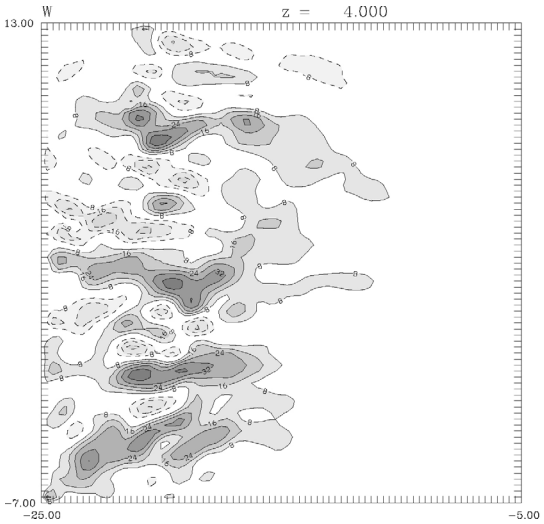

a) 4.0 km AGL at 0014 UTC (contour interval 8.0 m s^{-1}).

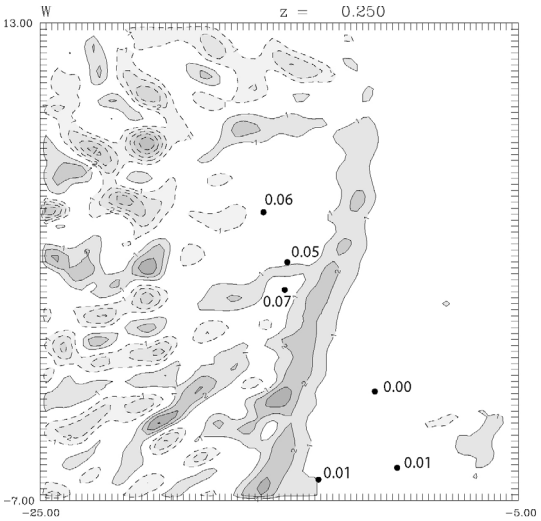

b) 0.25 km AGL at 0014 UTC (contour interval 1.0 m s^{-1}).

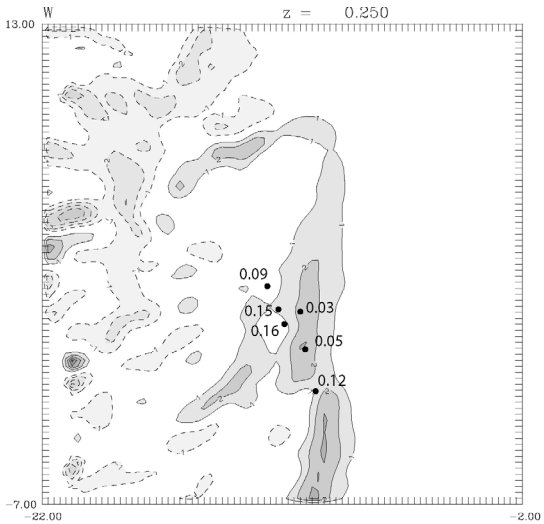

c) 0.25 km AGL at 0020 UTC (contour interval 1.0 m s^{-1}).

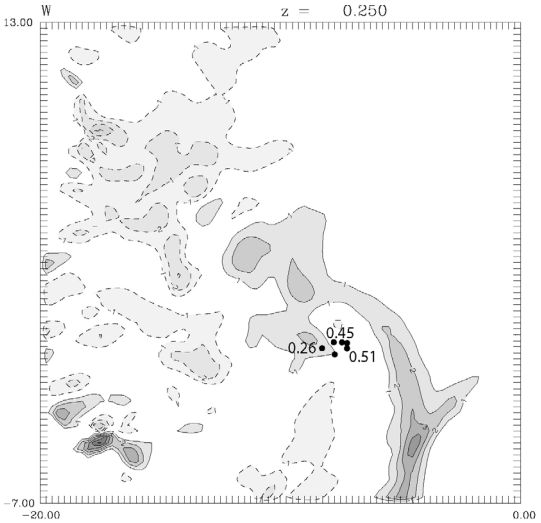

d) 0.25 km AGL at 0026 UTC (contour interval 1.0 m s^{-1}).

Figure 2. Vertical velocity (contours and shading; negative values are indicated by dashed contours and lighter shading) in the dual-Doppler syntheses. Distances (km) are relative to DOW2. Locations (heights in km AGL) of parcels that end in a 1 km wide circle around the tornado at 0.25 km AGL at 0028 UTC are shown in the plots at 0.25 km.

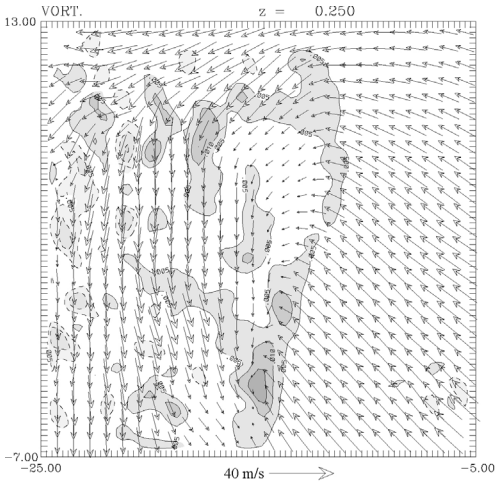

a) 0014 UTC

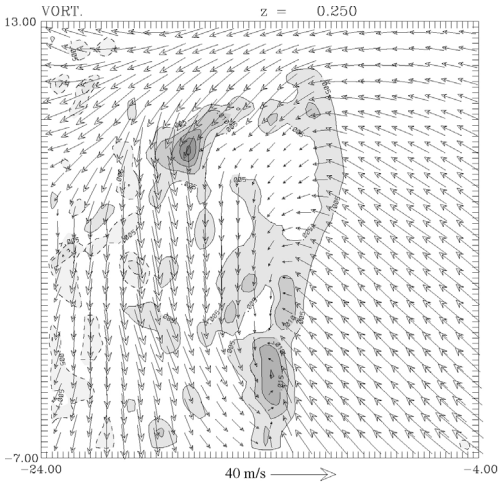

b) 0016 UTC

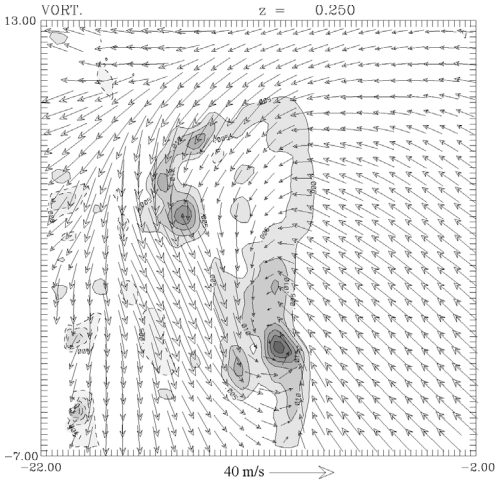

c) 0020 UTC

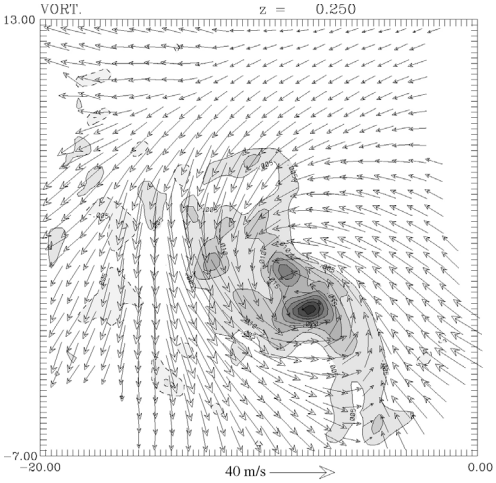

d) 0026 UTC

Figure 3. Horizontal storm-relative wind (vectors, plotted at every third grid point in each direction) and vertical vorticity (contours and shading at intervals of 0.005 s^{-1}) at 0.25 km AGL.

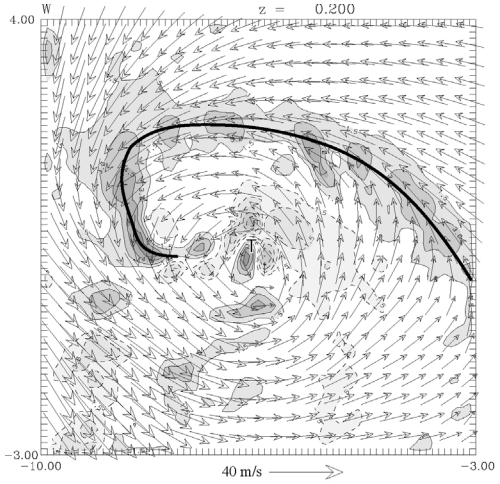

a) Horizontal storm-relative winds and vertical velocity (contours and shading at intervals of 1.5 m s^{-1}).

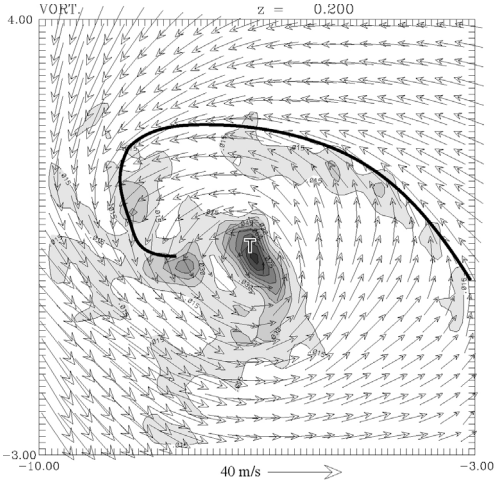

b) Horizontal storm-relative winds and vertical vorticity (contours and shading at intervals of 0.015 s^{-1}).

Figure 4. Detailed view of the tornadic region at 0.2 km AGL at 0028 UTC.